

# Portable Electromagnetic Field Applicator for Magnetic Hyperthermia Experiments

S.A. González, E.M. Spinelli and A.L. Veiga  
Dto. de Electrotecnia, Facultad de Ingeniería  
UNLP, La Plata, Argentina  
LEICI, CONICET

D.F. Coral, M.B. Fernández van Raap,  
P. Mendoza Zélis, G.A. Pasquevich and F.H. Sánchez  
Dto. de Física FCE-UNLP, La Plata, Argentina  
IFLP, CONICET

**Abstract**—We present a device based on a parallel LC resonant circuit optimized to generate alternating magnetic fields of 100 kHz frequency and amplitude adjustable from 2 to 15 kA/m. It is suitable for research aimed to the development of new nanotherapies that involve the use of magnetic materials and alternating magnetic field for fighting cancer, like magnetic hyperthermia and drug and gene delivery triggered by magnetic stimuli. The equipment is portable, air-cooled, versatile and functional to allow experimentation with materials, *in vitro* and *in vivo*. In addition, the design guarantees environmental bioterium conditions (ventilation, light, noise, humidity and temperature) for *in vivo* and of cell culture conditions (pH, temperature, osmotic pressure, partial pressure of O<sub>2</sub> and CO<sub>2</sub>) required for *in vitro* experiments.

**Index Terms**—RF; AC magnetic field; hyperthermia; magnetic nanoparticles.

## I. INTRODUCTION

New nanotherapies using magnetic nanoparticles (MNPs) and alternating magnetic field (AMF) in the radiofrequency range include magnetic hyperthermia (MH) [1] and heat-inducible targeted delivery of oncological drugs [2] or genes [3]. The MH oncologic therapy is based on the ability of the MNPs to selectively induce carcinoma-cell death upon exposure to an AMF. Carcinoma-cells activate the apoptosis mechanism when the tumor temperature is raised between 42 – 45°C, while necrosis mechanism activates in the range 45 – 50°C. MH therapy is already under clinical trials [4] in a unique active applicator working at 100 kHz and magnetic field strength adjustable from 2 to 15 kA/m.

Intelligent drug delivery uses stimuli responsive materials. Thermo-sensitive magnetic nanocarriers are designed to retain their payloads around the physiological temperature of 37°C, and release the payloads rapidly when temperature is increased above 40 – 45°C using AMFs. Finally, AMF activation of target cells to trigger specific gene expression *in vivo* is becoming a useful research tool and a potential means to control gene expression in clinical settings [5]. This overview indicates a need of specialized instrumentation to support research in the materials, *in vitro* and *in vivo* in controlled conditions.

In general, the design of the equipment used for these purposes includes a water-refrigerated hollow copper pipe wound around a cylindrical free space (where the sample is placed for treatments), being this coil a part of the resonant

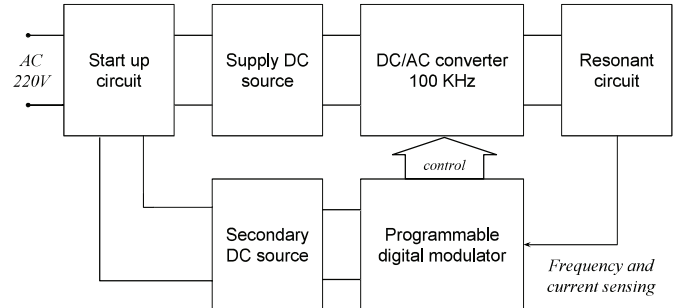


Fig. 1. Block diagram of the electrical circuit.

circuit. Water refrigeration is needed to avoid sample heating [6], making the equipment large, heavy and dependent on the availability of water free of harmful impurities and dependent of a specified supply pressure. Therefore this kind of equipment is not portable. This is a complication, since therapeutic trials are carried out in laboratories optimized for this purpose, where bioetic regulations are satisfied. These laboratories are often located in biology, medicine and even in health centers. It is therefore extremely advantageous to have a robust, small size applicator that can be transported to the application place without requiring specialized installation. To this end, it must be supplied with household voltage without any other additional cooling equipment, such as free water or compressed air.

Here, we described a portable applicator built and tested for research in materials and for *in vitro* and *in vivo* experiments. The device works at a field frequency of 100 kHz and variable amplitude between 2 y 15 kA/m, i.e in the range of clinical applicability [4].

## II. ELECTRONIC DESIGN

The proposed power conversion system is shown in Fig. 1. It consists of an LC resonant network, used to establish the magnetic-induction field and a DC/AC converter, both coupled by a high frequency insulator transformer. The inverter is powered by an unregulated DC source from a single phase diode bridge rectifier with filtering. The system is completed by a control circuit that fixes the operating frequency. In addition, auxiliary power supplies, start-up and protection circuits were designed. The digital interface implemented with

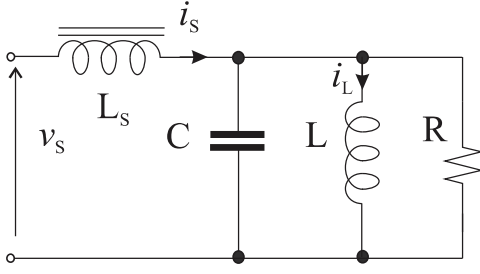


Fig. 2. Proposed L-LC network.

FPGA technology allows the operator to define field amplitude and frequency. In the next subsections, the resonant network and power electronics selection are described.

#### A. Resonant Network

The need to establish a high value magnetic field, that is uniformly distributed and confined to a particular space, requires a resonant network with high quality factor  $Q$ . Several resonant networks [7] can be used, but the serial and parallel topologies are best suited to the imposed needs. A resonant circuit with high  $Q$  involves small losses, in consequence high currents and voltages on  $L$  and  $C$  components. The series network has the advantage of not allowing a static magnetic field on the inductor due to the presence of the capacitor. But, with a high value of  $Q$  it requires an extremely low voltage and a very high value of the current that must be supplied by the power electronics. On the contrary, the parallel resonant network requires a low current and very high voltage supply. So, the parallel resonant circuit is the best solution for this application due to the low amplitude current demanded to the power electronics [8].

Different techniques can be used to develop a current source supply [9], [10]. In this case, the simplest technique is to use an L-LC network as shown in Fig.2 [11], [12]. Output voltage of the power electronics ( $v_s$ ) in series with  $L_s$  inductor adjusts the current supply at the LC parallel resonant circuit. When the quality factor is high, the relationship between the resonant currents  $i_L$  and  $i_s$  is given by:

$$\frac{i_s}{i_L} \simeq \frac{1}{Q} = \frac{R}{\omega_0 L} \quad (1)$$

with  $\omega_0^{-1} = \sqrt{LC}$  if  $L \ll L_s$ .

#### B. Power Electronics and control

The DC/AC power converter is the voltage supply of the L-LC network. There is a wide variety of topologies used for induction heating. Its choice depends on the power level and the precision required for the magnetic field [8]. In particular, hyperthermia treatments require very stable field amplitude and frequency. Therefore, a full-bridge converter was chosen, as presented in Fig. 3. This topology allows the control of both variables. The stability of the operating frequency is obtained by a phase locked loop circuit (PLL), on one branch of the converter. On the other branch, the control of the field

amplitude is performed by phase shifting the signal of the opposite branch. The field amplitude is measure and compared with a reference value  $H_{ref}$ . Then, the output signal of the proportional-integral controller (PI) enters to a modulator that introduces a phase shift between both sides of the inverter. The signal output of the PLL ( $PLL_{output}$ ) synchronizes a ramp generator. Then the saw-tooth voltage is compared with the PI signal output. The toggle flip-flop changes state in each comparison. Thus, the AC output of the converter is a width modulated voltage pulse, modulated by the required field amplitude  $H_{ref}$ .

### III. RESONANT CIRCUIT DESIGN

The resonant circuit is composed of a custom air core inductor in parallel with a commercial high-Q capacitor. The interior of the air core inductor is used as the treatment area (housing). It is designed to hold the full body of the animal. The capacitor is a commercial 50 nF (10%) CELEM CSP120/200 [13], which dimensions (35x35x30.2 mm) and weight (0.17 kg) are suitable for this application. It can handle up to 1000 Vrms sinusoidal voltage, which represents a limitation for the design. Maximum current is 200 Amperes, well above the requirements. Measured at 100 kHz using GW-Instek 818 LCR Meter the capacitance resulted 50.098 nF and the dissipation factor 0.0012 ( $1/Q$ ).

The inductor geometry minimizes the current necessary to obtain the required magnetic field. The inductor design aims to reduce the power loss achieving increased efficiency, along with the elimination of water cooling systems. Forced air cooling provides portability and operation of the equipment in the field.

An optimized electric design of the inductor was performed to reduce losses and to avoid overheating and temperature increase. This enables to keep the interior of the receptacle at room temperature by forced air circulation. The main electrical criteria used in the design of inductor field were: a) air core solenoid whose geometry provides a zone of homogeneous field in the center; b) single layer winding to facilitate heat dissipation; c) multi-wire conductor to increase the effective section due to the skin effect of the current at the operating frequency.

The conductor used for the inductor is composed of 40 glazed copper wires of 0.25 mm diameter, resulting in a conductor of an overall diameter of approximately 2 mm. On a cylindrical acrylic support of 55 mm of inner diameter (3 mm wall) 35 turns of the mentioned conductor were coiled in one layer, resulting in a length of about 70 mm. The receptacle total volume is 170 cm<sup>3</sup>, with 70 cm<sup>3</sup> of uniform field. The resulting inductance was 47.6 uHy with a  $Q$  of 234 at the operating frequency (a resistance less than 0.12 ohm). The capacitor and the inductor were mounted using copper bars and carefully isolated from the rest of the equipment. The measured resonant frequency resulted 103.1 kHz.

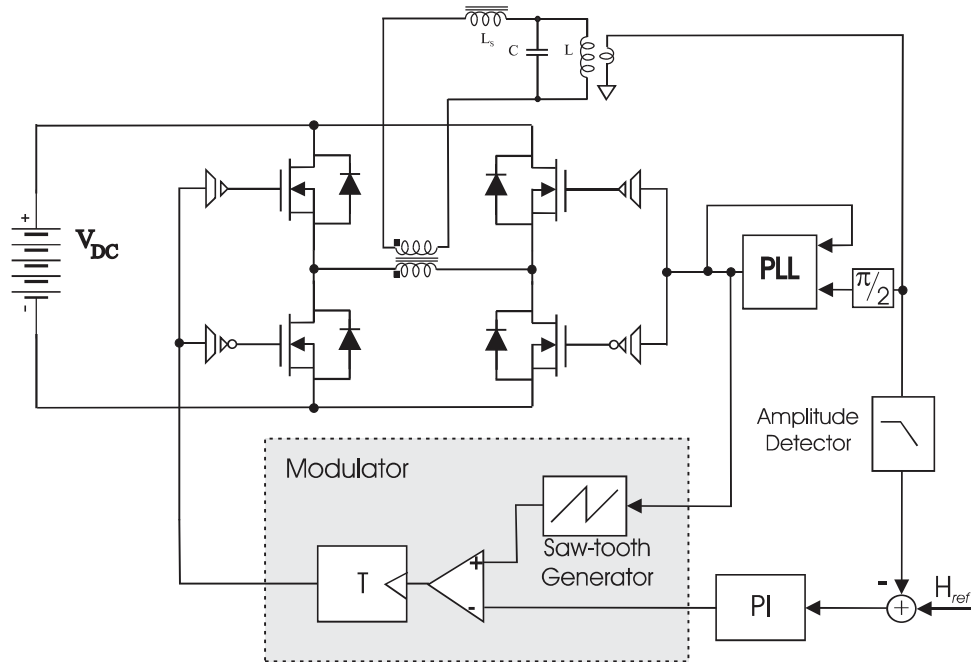


Fig. 3. Power electronics and control.

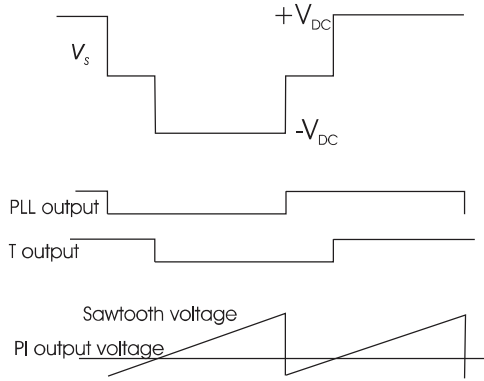


Fig. 4. Timing diagram.

#### IV. COOLING SYSTEM DESIGN

The air flow was designed to remove the heat generated by the coil and other elements, in order to maintain room temperature in the receptacle. To this end, a forced air flow is established with a single fan in several concentric annular sections: one for cooling the outside of the inductor and the other for cooling the space between the receptacle and the inductor (see Fig.5). A nozzle was designed to promote cooling and the adequate conditions of temperature and receptacle ventilation, including removable support to enter the animal under treatment. The receptacle holder was designed to ensure the rigidity, therefore minimizing conductive heat transfer from the inductor.

The receptacle is rotatable such that in its horizontal position can accommodate the animal laying in ventral or dorsal position. In its upright position holds liquid suspensions in

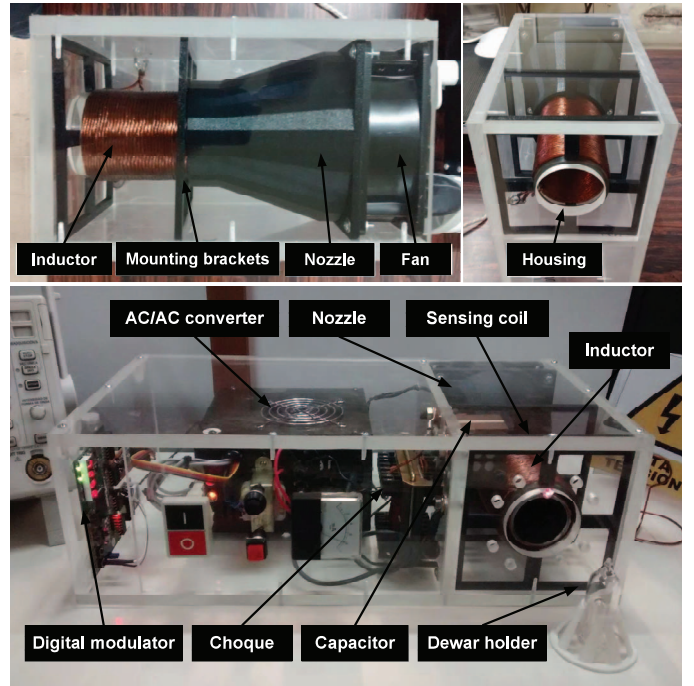


Fig. 5. Prototype.

adiabatic Dewar and culture cells in Petri dish of 35 by 10 mm size. Multiple supports (adapters) that ensure the sample centering inside inductor coil were designed (see Fig.5). The cabinet design respects ergonomic requirements, so that the receptacle is at the level of a standing user.

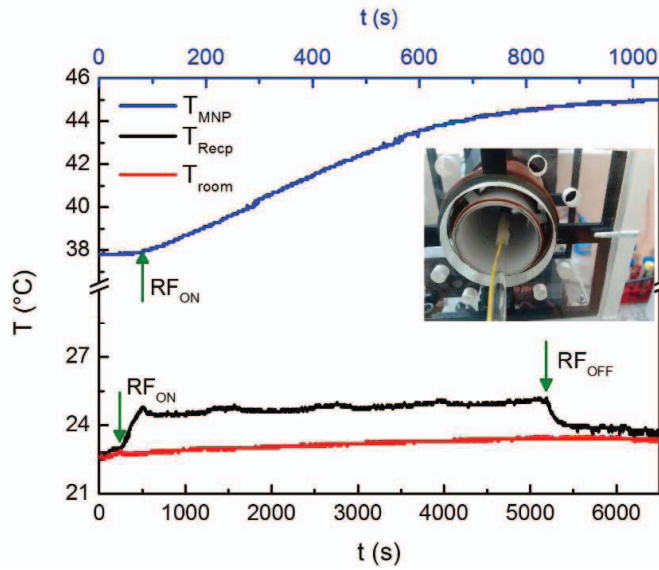


Fig. 6. Temperature profile.

## V. EXPERIMENTAL VERIFICATION

In order to characterize the thermal performance of the equipment during measurements at maximum field amplitude (Fig.6), the temperature inside the receptacle was registered with an optical fiber sensor as showed in photograph in Fig.6. The sensor was connected to a calibrated signal conditioner (Neoptix) of  $\pm 0.1^\circ\text{C}$  accuracy. First, the receptacle temperature profile ( $T_{Recp}$ ) during the operating time is sensed and compared with room temperature ( $T_{room}$ ). When the RF field is turned on ( $RF_{ON}$  arrow), the internal temperature increases around  $2.0 \pm 0.1^\circ\text{C}$  from  $T_{room}$  and this increment is hold over time. After turning off the field ( $RF_{OFF}$  arrow) the room temperature is recovered, indicating the fan cooling efficiency to avoid the receptacle overheating. In a second experiment, the heating of a magnetic nanoparticles set fixed in agarose ( $T_{MNP}$ ) is studied. Before experiment, a thermal bath was selected at  $38^\circ\text{C}$  to simulate the mouse corporal temperature. When the RF field is turned on at maximum power, the temperature increases until  $45^\circ\text{C}$ , reaching the temperature needed to produce cellular apoptosis. It is important to note that the ability to reach the apoptotic temperature depends on the physical-chemical properties of the magnetic nanoparticles and on the RF-field amplitude and frequency.

## VI. CONCLUSIONS

The design, implementation and testing of a portable applicator of an alternating magnetic field in the RF range for magnetic hyperthermia was shown. It is intended for research in materials and for *in vitro* and *in vivo* experiments. A careful design of electrical an refrigeration parameters allowed to put aside water cooling and other voluminous characteristics, usual in this kind of equipment, while still operating in the range of clinical applicability. A prototype was built and tested

## REFERENCES

- [1] S. Dutz, R. Hergt. Nanotechnology, Magnetic particle hyperthermia-a promising tumour therapy? 2014, 25,452001.
- [2] Maribella Domenech, Ileana Marrero-Berrios, Madeline Torres-Lugo, and Carlos Rinaldi, Lysosomal Membrane Permeabilization by Targeted Magnetic Nanoparticles in Alternating Magnetic Fields. ACSNano 2013,7(6) 5091 -5101
- [3] Masaki Yamaguchi, Akira Ito, Akihiko Ono, Yoshinori Kawabe, and Masamichi Kamiyama Heat-Inducible Gene Expression System by Applying Alternating Magnetic Field to Magnetic Nanoparticles ACS Synth. Biol., 2014, 3 (5), pp 273279. DOI: 10.1021/sb4000838
- [4] Klaus Maier-Hauff, Frank Ulrich,Dirk Nestler, Hendrik Niehoff, Peter Wust, Burghard Thiesen, Helmut Orawa, Volker Budach, and Andreas Jordan. Efficacy and safety of intratumoral thermotherapy using magnetic iron-oxide nanoparticles combined with external beam radiotherapy on patients with recurrent glioblastoma multiforme. J Neuro oncol. 2011 Jun; 103(2): 317324. doi: 10.1007/s11060-010-0389-0
- [5] Stanley, S. A., Gagner, J. E., Damanpour, S., Yoshida, M., Dordick, J. S., and Friedman, J. M. (2012) Radio-wave heating of iron oxide nanoparticles can regulate plasma glucose in mice. Science 336, 604608.
- [6] E Garaio, J M Collantes, F Plazaola, J A Garcia and I Castellanos-Rubio A multifrequency eletromagnetic applicator with an integrated AC magnetometer for magnetic hyperthermia experiments Meas. Sci. Technol. 25 (2014) 115702
- [7] M. T. Outeiro, G. Buja and D. Czarkowski, "Resonant Power Converters: An Overview with Multiple Elements in the Resonant Tank Network," in IEEE Industrial Electronics Magazine, vol. 10, no. 2, pp. 21-45, Summer 2016.
- [8] O. Luca, P. Maussion, E. J. Dede and J. M. Burdo, "Induction Heating Technology and Its Applications: Past Developments, Current Technology, and Future Challenges," in IEEE Transactions on Industrial Electronics, vol. 61, no. 5, pp. 2509-2520, May 2014.
- [9] P. Dawson and P. Jain, "A comparison of load commutated inverter systems for induction heating and melting applications," in IEEE Transactions on Power Electronics, vol. 6, no. 3, pp. 430-441, Jul 1991.
- [10] S. A. Richter, P. Gaertner, D. Hirschmann and R. W. De Doncker, "Design of a PWM current source rectifier for high power induction melting applications," Power Electronics and Applications, 2009. EPE09. 13th European Conference on, Barcelona, 2009, pp. 1-9.
- [11] J. M. Espi-Huerta, E. J. Dede Garcia Santamaria, R. Garcia Gil and J. Castello-Moreno, "Design of theL-LCResonant Inverter for Induction Heating Based on Its Equivalent SRI," in IEEE Transactions on Industrial Electronics, vol. 54, no. 6, pp. 3178-3187, Dec. 2007.
- [12] Chudjuarjeen, A. Sangswang and C. Koompai, "An Improved Resonant Inverter for Induction-Heating Applications With Asymmetrical Control," in IEEE Transactions on Industrial Electronics, vol. 58, no. 7, pp. 2915-2925, July 2011.
- [13] <http://www.celem.com/>